N O T I C E

THIS DOCUMENT HAS BEEN REPRODUCED FROM MICROFICHE. ALTHOUGH IT IS RECOGNIZED THAT CERTAIN PORTIONS ARE ILLEGIBLE, IT IS BEING RELEASED IN THE INTEREST OF MAKING AVAILABLE AS MUCH INFORMATION AS POSSIBLE

A THERMALIZED ION EXPLOSION MODEL FOR HIGH ENERGY SPUTTERING AND TRACK REGISTRATION[†]

L. E. SEIBERLING, J. E. GRIFFITH and T. A. TOMBRELLO

W. K. Kellogg Radiation Laboratory

California Institute of Technology, Pasadena, California 91125

ABSTRACT

A velocity spectrum of neutral sputtered particles as well as a low resolution mass spectrum of sputtered molecular ions has been measured for 4.74 MeV $^{19}F^{+2}$ incident on UF_4. The velocity spectrum is dramatically different from spectra taken with low energy (keV) bombarding ions, and is shown to be consistent with a hot plasma of atoms in thermal equilibrium inside the target. We propose a "thermalized ion explosion" model for high energy sputtering which is also expected to describe track formation in dielectric materials. The model is shown to be consistent with the observed total sputtering yield and the dependence of the yield on the primary ionization rate of the incident ion.

[†]Supported in part by the National Aeronautics and Space Administration [NGR 05-002-333], the National Science Foundation [PHY79-23638] and the Department of Energy [EX-76-G-03-1305].

ONE OF THE BAND AID PREPRINT SERIES IN ATOMIC & APPLIED PHYSICS

April 1980

A THERMALIZED ION EXPLOSION MODEL FOR HIGH ENERGY SPUTTERING AND TRACK REGISTRATION[†]

L. E. SEIBERLING, J. E. GRIFFITH and T. A. TOMBRELLO

W. K. Kellogg Radiation Laboratory

California Institute of Technology, Pasadena, California 91125

ABSTRACT

A velocity spectrum of neutral sputtered particles as well as a low resolution mass spectrum of sputtered molecular ions has been measured for 4.74 MeV $^{19}F^{+2}$ incident on UF_4. The velocity spectrum is dramatically different from spectra taken with low energy (keV) bombarding ions, and is shown to be consistent with a hot plasma of atoms in thermal equilibrium inside the target. We propose a "thermalized ion explosion" model for high energy sputtering which is also expected to describe track formation in dielectric materials. The model is shown to be consistent with the observed total sputtering yield and the dependence of the yield on the primary ionization rate of the incident ion.

[†]Supported in part by the National Aeronautics and Space Administration [NGR 05-002-333], the National Science Foundation [PHY79-23638] and the Department of Energy [EX-76-G-03-1305].

ONE OF THE BAND AID PREPRINT SERIES IN ATOMIC & APPLIED PHYSICS

April 1980

1. INTRODUCTION

In an earlier paper,[1] we presented data on uranium sputtered from a uranium tetrafluoride target. The beams employed were heavy ions with energies near the peak in the electronic stopping power. Our purpose was to test a prediction by Haff[2] that good insulators may exhibit large sputtering yields associated with track formation when bombarded with energetic heavy ions. Very large sputtering yields were found which could not be explained by standard sputtering theory.[3] Other investigators have seen enhanced sputtering from a number of insulating targets when bombarded under similar conditions.[4-9] Metals, however, do not appear to show the enhanced sputtering effect.[10,11] These data support the suggestion by Haff, that enhanced sputtering due to energetic heavy ion bombardment and track formation arise from the same mechanism. This mechanism is generally thought to be either thermal in nature,[4,7,8,12] with an electron-phonon interaction supplying heat to the lattice atoms, or collisional[5,6,13] with an "ion-explosion" leading to a weak collision cascade.

In this paper we shall attempt to determine which of the above mechanisms is responsible for enhanced sputtering in UF_4. An energy spectrum of sputtered particles presented in Reference 1 was fit to a curve of the form

$$S(E) \propto E/(E+E_b)^n. \qquad (1)$$

This function is expected to describe collision cascade sputtering typical of low energy ion bombardment. E_b is the surface binding energy and n is generally close to 3 (Reference 14). However, when fit to our energy spectrum taken with 4.74 MeV $^{19}F^{+2}$ ion bombardment, a least squares analysis gave values of E_b = 1.2 eV and n = 6.1. The large value of n reflects a very rapid decrease in the yield with increasing energy. This would suggest

an extremely weak collision cascade or could be indicative of a thermal spike. Another time-of-flight (TOF) spectrum which incorporates a number of improvements is presented here. The resolution has been improved by a factor of two, more data were accumulated which decreased the statistical uncertainty, and a voltage drop between the target and detector was used to separate the charged from the neutral particles. This last change also allowed us to separate charged molecular clusters having different masses. The neutral particle data are converted to a velocity spectrum and fit to a curve which represents a Maxwell-Boltzmann velocity distribution inside the target. Based on these data, we propose a thermal model of high energy sputtering of dielectrics and suggest a mechanism for attaining thermal equilibrium inside the target which utilizes the ion-explosion concept. An explicit expression for the total sputtering yield is calculated and compared with our data.

2. EXPERIMENTAL RESULTS

A mechanical TOF spectrometer developed by Weller and Tombrello[15] was used to measure the TOF spectrum of uranium sputtered from UF_4 by 4.74 MeV $^{19}F^{+2}$. The experimental arrangement is illustrated in Figure 1. The sputtered particles which are emitted normal to the target surface, travel back along the beam line and are collected on a rotating aluminum wheel. Zero time-of-flight corresponds to the center of the slit in the rotating wheel, which is used to chop the incident beam. After the sputtered particles are collected, a freshly cleaved piece of mica is placed against the wheel, and the resulting layered package is exposed to a flux of thermal neutrons. The ^{235}U is then detected by observing neutron induced fission fragment tracks in the mica. This sensitive technique for detecting extremely

low sputtering yields of ^{235}U is described by Gregg et al. in Reference 16.

A detailed description of the experimental apparatus and procedure is given in References 1 and 15 and only the modifications will be presented here. The target, which consists of an evaporated UF_4 film approximately 5000 Å thick on a polished copper backing, was biased at +100 volts during the run. A grounded steel disc with a circular aperture through which the ion beam and sputtered particles traveled, was placed approximately 4 cm in front of the target. Thus, the sputtered ions were rapidly accelerated to 100 eV before drifting the remaining distance (~ 70 cm) to the collector wheel. The 100-volt bias was chosen as a result of two competing effects. A large voltage was needed to give the sputtered ions (which leave the target with a few eV or less) sufficient rigidity to withstand small magnetic fields along the flight path. Magnetic shielding was used to reduce ambient magnetic fields to less than 0.1 Gauss; however, the sputtered ions were still bent several mm over a flight path of 75 cm. The resolution of our spectrometer decreases very rapidly with decreasing TOF, so that with too large a voltage adjacent clusters could not be resolved. The 100-volt bias was thus a compromise between particle rigidity and resolution. The overall resolution of the spectrometer was improved by reducing the width of the rotating and fixed slits by a factor of two.

In Figure 2 we show the full TOF spectrum. The region between $2 < t/28 \times 10^{-6}$ sec < 16 contains the charged particles. In the inset we have expanded the region of sharp mass peaks and indicated the expected location of various molecular ions. Each of the molecules is assumed to have a + 1 charge. The dashed line under the first peak indicates the limiting resolution of our spectrometer due to the finite width of the fixed and rotating slits. A higher resolution spectrum is clearly needed in order

to determine the identity and abundance of each molecular species.

The slight deflection of the sputtered ions due to ambient magnetic fields has made the relative peak heights in Figure 2 uncertain to about ± 10%. The ratio of sputtered ions to neutrals inferred from Figure 2 is roughly 20%; however, this should be taken as an upper limit because of electrostatic focusing. Since our detector is only sensitive to individual uranium atoms, the molecules in the second peak are counted twice, the third peak three times, etc. For this reason, the area in the second peak should be divided by two and the third peak by three in order to obtain the number of clusters in each peak.

We now turn our attention to the neutral particles and investigate the possibility that they arise from a thermal mechanism. Perhaps the simplest starting point is to assume that a cylindrical region of constant radius r_0 along the incident ion path contains a hot plasma at a temperature T_0 (T_0 is the kinetic temperature of the atoms, assumed to be in thermal equilibrium). We also assume that the temperature $T = T_0$ is constant from time $t = 0$ to $t = \tau$ and that $T = 0$ for $t > \tau$. The basis for these assumptions will be discussed further in the next section. The atoms inside this cylinder have a Maxwell-Boltzmann velocity distribution[17] given by

$$F(v)dv = n(M/2\pi kT)^{3/2} 4\pi v^2 \exp(-Mv^2/2kT)dv \qquad (2)$$

where v is the magnitude of the velocity, n is the number density of target particles each of which has a mass M, and k is the Boltzmann constant, $k = 8.6 \times 10^{-5}$ eV/°K. Let the surface of the target have a step potential E_b and consider the particles which cross this surface. If the resultant velocity outside of the target is v' and θ is the angle between $\vec{v}'$ and the normal to the target surface ($v' = |\vec{v}'|$), then the flux of atoms sputtered

into solid angle $d\Omega$ at θ with resultant velocity in (v', dv') is

$$\varphi(v', \Omega)dv'd\Omega = n(M/2\pi kT)^{3/2} \exp(-E_b/kT) \exp(-Mv'^2/2kT) \cos\theta\, v'^3\, dv'd\Omega. \quad (3)$$

The number of atoms sputtered into our detector at $\theta = 0$ and with solid angle Ω_d with v' in (v', dv') is

$$N(v')dv'\Omega_d = \pi r_0^2 \tau n(M/2\pi kT)^{3/2} \exp(-E_b/kT) \exp(-Mv'^2/2kT)\, \Omega_d v'^3 dv' \quad (4)$$

or

$$N(v)dv \propto v^3 \exp(-Mv^2/2kT)dv \quad (5)$$

where the primes have been dropped in the last expression.

In Figure 3 we show the data plotted as a velocity spectrum with arbitrary normalization. The errors shown arise from counting statistics. A background subtraction has been made as indicated by the dashed line in Figure 2. This line represents the contribution to the spectrum due to very slow particles which wrap around to the beginning of the collector wheel on the next cycle. The line was calculated assuming the data follow the dashed line of Figure 3 at low velocities. The solid curve is a two parameter fit with Equation (5). The parameters are the normalization (which is discussed further in section 4) and the ratio M/T. A value of 235 amu for M gives T = 3500 ^{o}K. Thus the solid curve assumes that only single uranium atoms evaporate from the surface. The dashed curve of Figure 3 is a superposition of two curves, each having the form of Equation (5), assuming that 20% of the uranium comes off as U_2 molecules and 80% as U atoms. The temperature in this case is 4100 ^{o}K and is the same for both species. The purpose of the dashed curve is to show the effect of adding an arbitrary (although

reasonable) amount of U_2 to the spectrum. For the sake of simplicity, in further calculations we shall assume that only U atoms are present and that T = 3500 ^{o}K. Encouraged by the fit of Equation (5) to our data, and the reasonable value of T (the melting temperature of UF_4 is 1309 ^{o}K), we shall proceed in the next sections to investigate further aspects of a thermal model.

3. LOCAL THERMAL EQUILIBRIUM

Is it reasonable to expect that atoms near the path of the incident ion reach a condition of local thermodynamic equilibrium (LTE)? When an ion with an energy of approximately 1 MeV/amu enters a solid, virtually all of its energy loss goes to the electrons of the medium. These electrons must give their energy to the lattice atoms more quickly than the energy is thermally conducted away. The most efficient way for electrons to transfer energy to atoms via collisions is for each electron to suffer a head-on elastic collision with an atom each time it travels one lattice spacing. This is, of course, an unrealistic assumption; most of the electron-atom collisions correspond to small angle scattering of the electrons. However, we do in this way establish a lower limit on the time required to transfer the electron's energy into thermal motion. We assume that the recoil electron shares its energy rapidly with other bound electrons until it is degraded to a few eV. At this point the electron can no longer ionize an atom, and transfer of kinetic energy to the atom becomes important. In UF_4, one lattice spacing is d = 4.3 Å; therefore, the time between collisions is $d/v \sim (4.3 \times 10^{-8}/6 \times 10^{7})$ sec = 7×10^{-16} sec where 6×10^{7} cm/sec is the velocity of a 1 eV electron. The fraction of energy transferred to a mass M by a mass m (for $m \ll M$) in a single head-on

elastic collision is $4m/M = 9.3 \times 10^{-6}$ for $M = 235$ amu and m equal to the mass of an electron. The time for an electron to transfer its energy to a ^{235}U atom is thus:

$$t_{ea} \geq (M/4m)(d/v) = 7.5 \times 10^{-11} \text{ sec.}$$

This time should be shorter than or comparable to the time in which a significant fraction of the heat is conducted away, t_{hc}. Solving the diffusion equation in a cylindrical geometry with constant thermal conductivity κ and heat capacity C we get[18]

$$T(r,t) = (\epsilon/4\pi\kappa t) \exp(-C\rho r^2/4\kappa t) \qquad (6)$$

for a line source of energy density ϵ per unit length at $r = 0$ and $t = 0$. ρ is the target mass density and T is the temperature. For $t > C\rho r^2/4\kappa$ the temperature begins to decrease rapidly. Therefore we take

$$t_{hc} = r_0^2/4K,$$

where $K = \kappa/C\rho$ is the thermal diffusivity and r_0 is the radius of the thermal spike. For UF_4 at $60^\circ C$, $K = 8 \times 10^{-3}$ cm^2/sec. Using $r_0 = 20$ Å (this will be justified in section 4), we have

$$t_{hc} = 1.3 \times 10^{-12} \text{ sec.}$$

This is over fifty times smaller than t_{ea}; thus, heating of the lattice through electron-phonon interactions does not appear to be an efficient process in UF_4. Actually the situation is even worse than this. Since the atoms are bound in a lattice, they cannot accept arbitrarily small amounts of energy. The maximum energy which can be transferred to an atom by an

electron of a few eV is much smaller than the lowest vibrational energy level of the typical atom in a crystal lattice.

Another, possibly faster, method of heat transfer into the lattice is through "ion explosions." If neighboring lattice atoms are ionized by the passing incident ion and if they are not neutralized too rapidly, they will repel each other, gaining a substantial amount of kinetic energy. If two adjacent molecules are triply ionized, for example, and recoil from one lattice spacing to three before colliding with other atoms, they will each gain a kinetic energy equal to

$$V = \tfrac{1}{2} (3e)^2 (1/d - 1/3d) = 10.2 \text{ eV}.$$

When these molecules collide with other stationary molecules, they will transfer approximately one half of their energy per collision. After a few collisions, a condition approaching LTE will be reached if heat is conducted away slowly compared to the collision time. We estimate the collision time, t_{aa}, to be the time for a 1 eV ^{235}U atom to travel one lattice spacing

$$t_{aa} = (4.3 \times 10^{-8}/9 \times 10^{4}) \text{ sec} = 4.8 \times 10^{-13} \text{ sec}.$$

This is several times smaller than t_{hc} and over two orders of magnitude smaller than t_{ea}. The time scales suggest that it may be possible to achieve LTE in a region of radius $\sim r_0$ for a time $\sim r_0^2/4K$.

The fact that t_{hc} and t_{aa} are of the same order of magnitude suggests that the thermal diffusivity may be responsible for quenching sputtering and track registration in certain materials. Sapphire, which has a very high thermal conductivity but a low electrical conductivity, has never been observed to register tracks.[19] Increasing electrical conductivity could also quench the sputtering or track forming process. This effect has been

observed[20,11] and is attributed to mobile electrons which neutralize the ions before they can repel each other.

4. THE SPUTTERING YIELD

From Equation (3), the number of atoms sputtered into solid angle $d\Omega$ at θ with velocity in (v,dv) is

$$S(v,\Omega)dvd\Omega = \varphi(v,\Omega)(\pi r_0^2)(r_0^2/4K)dvd\Omega. \tag{7}$$

Here we assume that the temperature in the spike quickly reaches its equilibrium value and as the cylinder loses heat, its radius contracts while the temperature stays roughly constant. The average spike radius is thus given by r_0. Integrating over solid angle and velocity gives the total sputtering yield,

$$S = \iint S(v,\Omega)dvd\Omega = n(\pi r_0^4/4K)\ (kT/2\pi M)^{\frac{1}{2}} \exp(-E_b/kT). \tag{8}$$

We may use this formula with measured values of S, T and E_b in order to deduce a value for r_0. The spike temperature was measured for 4.74 MeV $^{19}F^{+2}$ ions and was found to be 3500 ^{o}K with M = 235 amu. The same bombarding ions gave a sputtering yield of approximately 5.5 uranium atoms per incident ion (see Figure 4). The binding energy, E_b = 0.71 eV, is obtained from a fit of Equation (1) to an energy spectrum with 80 keV $^{20}Ne^{+}$ incident on a UF_4 target.[1] Substituted into Equation (8) these values of S, T and E_b give r_0 = 24 Å, which is consistent with the value of r_0 used in our calculation of t_{hc} and is also consistent with the observed radii of latent tracks.[20]

The temperature and radius of the spike are expected to depend on the electronic stopping power of the bombarding ion, dE/dx. A related quantity,

the primary ionization rate (denoted dJ/dx), has been found by Fleischer et al. to more accurately describe track registration thresholds.[21] It is defined as the number of ionizations caused directly by the incident ion per unit path length of the ion. Multiple ionizations are included but secondary ionizations due to scattered electrons are not. A theoretical expression for dJ/dx was presented by Bethe in 1930 (Reference 22) and for small velocity ($\beta \equiv v/c < 0.1$) reduces to:

$$dJ/dx = Z_e^2 (A/\beta^2) \ln(B\,\beta^2) \tag{9}$$

$$Z_e = Z\left\{1 - 10^{-(1/3)(137\beta/Z^{0.55})}\right\} \tag{10}$$

Equation (10) is due to Heckman et al.[23] with Z the atomic number of the incident ion. The constants A and B in Equation (9) depend on the material through which the ion passes and are difficult to measure or calculate for most solids. For this reason $dJ/dx(\beta)$ is rather uncertain in both magnitude and shape. We have chosen to fix B by fitting data taken from protons and electrons in argon,[24,25] which gives a value of $B = 2.1 \times 10^4$.

In order to obtain an expression relating T and r_0 to dJ/dx, we assume (for concreteness) that two ions of charge +N are created each lattice spacing, thus

$$dJ/dx = 2N/d.$$

If E_0 is the energy per atom in the spike due to the incident ion, then

$$(3/2)kT = E_0 + (3/2)kT_0$$

with T_0 the ambient target temperature. Further,

E_0 = (kinetic energy per primary recoil)

× (number of primary recoils per lattice spacing)

+ (number of atoms in the spike per lattice spacing)

$$= \left[\tfrac{1}{2}\,(dJ/dx)^2(de/2)^2(1/d - 1/3d)\right](2/d)/(n\pi r_0^{\,2})$$

$$= \frac{e^2}{6n\pi r_0^{\,2}}\left(\frac{dJ}{dx}\right)^2 \propto \left(\frac{dJ/dx}{r_0}\right)^2$$

which gives the desired relation:

$$kT = D\left(\frac{dJ/dx}{r_0}\right)^2 + kT_0 \qquad (11)$$

where D is a constant.

One further equation relating T, r_0 and dJ/dx is needed in order to obtain S in terms of dJ/dx alone. Two cases will be chosen which represent opposite extremes, with the understanding that the true situation lies somewhere between.

Case I: $r_0 \propto dJ/dx$

Here, the spike temperature is independent of dJ/dx, and the spike radius expands (contracts) as dJ/dx increases (decreases) to accommodate the changing energy deposition rate. This would occur if the spike temperature were determined only by physical or chemical properties of the target such as melting point, bond strength, etc. In this case we have

$$S \propto (dJ/dx)^4 \,. \qquad (12a)$$

Case II: r_0 = constant

Here, we have the spike radius determined by properties of the target while the spike temperature varies as $(dJ/dx)^2$ for $T_0 \ll T$. This case appears somewhat less likely and has the disadvantage that the binding energy, E_b,

cannot be factored out of the expression for S. In this case we have

$$S \propto dJ/dx \exp[-E_b r_0^2/D(dJ/dx)^2] \quad . \tag{12b}$$

D is fixed by defining a normalization for dJ/dx and solving Equation (11) for D, using T = 3500 ^{o}K and the value of dJ/dx at a fluorine energy of 4.74 MeV. Figure 4 shows sputtering yield values as a function of fluorine energy along with curves for case I, case II with E_b = 0.5 eV, and dE/dx for comparison. The numbers beside the data points indicate the incident fluorine ion charge state and the error bars correspond to the standard deviations of the measured yields in those cases for which more than one run was performed. Where no error bar is shown, only one run was made.

5. DISCUSSION

We have emphasized that the dependence of dJ/dx on ion velocity is highly uncertain, being very difficult to calculate or measure for an arbitrary solid. For this reason, a comparison of our model with sputtering yield data for a given ion at different velocities (such as in Figure 4) is of limited value. It would be more useful to compare data for different ions, each having the same velocity. In this case, $dJ/dx \propto Z_e^2$ with $Z_e(Z,\beta)$ empirically determined, as in Equation (10). Since dE/dx also scales as Z_e^2, this method of comparison does not distinguish between dJ/dx and dE/dx. This may be an advantage, however, as it is still a matter of some controversy which quantity (if either) is most relevant to the occurrence of an ion explosion.

In Table I we give sputtering yield predictions for a number of different ions with the same velocity (E/M = $\frac{1}{4}$ MeV/amu) for cases I and II of section 4. Also shown are measured yields due to Griffith.[1,10] The

calculated values have been normalized to best fit the measured values. The incident charge state of the beam is indicated in the cases where measurements were made; however, it has been shown to have a rather small effect on the total yield.[1] Case I is seen to fit the data well except for He^+ for which the measured value is uncertain to about a factor of two. The measured sputtering yields include both high energy sputtering and a small contribution from low energy (collision cascade) sputtering. Since the calculated yields account only for high energy sputtering, when they fall too low, disagreement with the measured values would be expected. Thus, collision cascade theory predicts a sputtering yield of $\sim 2 \times 10^{-4}$ for He^+ (Reference 10), so that the case II predictions are in agreement with the measured value while the case I prediction is not. It should be noted here that although $Z_e(Z,\beta)$ is a more accurately known function than $dJ/dx(\beta)$, several slightly different formulae exist for Z_e and these can differ by as much as 15% for $Z \gtrsim 20$. A 15% difference in Z_e leads to a factor of three difference in the yield calculated for case I. For this reason, sputtering yields for chlorine could not distinguish case I from case II, but yields for lithium or carbon probably could.

Although the thermalized ion explosion model presented in this paper describes high energy sputtering of UF_4 quite well thus far, more data are needed to determine if the same model can describe the sputtering of other target materials. Unfortunately, very few data exist at the present time which we feel are applicable to this model. Brown et al.[5] have measured the sputtering of ice with 1.5 MeV ^4He, ^{12}C and ^{16}O beams and with 1.5 MeV and 0.5 MeV ^1H. We display their results in Table II along with predictions of our model (case I) which have been normalized to best fit their data (see discussion below). It can be seen that our model fits remarkably well with

the ^{4}He, ^{12}C, and ^{16}O data but fits the ^{1}H data poorly. We feel this can be understood if one considers the ion explosion mechanism of heat transfer to the lattice. In order for an ion explosion to occur, one would need a minimum of one ionization per lattice spacing. In water, ~ 30 eV are needed to create one ion-electron pair, so that the minimum dE/dx needed to trigger an ion explosion would be ~ 30 eV per lattice spacing. The maximum dE/dx for the ^{1}H ions used by Brown et al. was 17.1 eV/(10^{15} molecules/cm^2) ~ 17 eV per lattice spacing. Thus our model would not be expected in its present form to apply to ice sputtering with protons. However, the excitation of higher vibrational modes of the water molecules caused by the proton's passage may drive a similar thermal mechanism even though no ion explosions are taking place.

It would be instructive at this point to estimate the spike radius for heavy ions on ice given the sputtering yields measured by Brown et al. Using a thermal diffusivity $K = 1.05 \times 10^{-2}$ cm^2/sec [for ice at 0°C (Reference 26)] a spike temperature of 800 °K (~ 3 times the melting point of ice, chosen in comparison with our UF_4 result) and a binding energy E_b = 0.5 eV (the sublimation energy of ice) one obtains the following spike radii:

$r_0 = 68$ Å for S = 10,

and

$r_0 = 193$ Å for S = 640.

These are not unreasonable values given the order of magnitude nature of the calculation. It thus appears that ice sputtering with heavy ions may also be explained with the thermalized ion explosion model, although more data are needed to confirm this in detail.

The virtue of our model is that concrete predictions can easily be made for comparison with experimental data. In addition to the sputtering yield

predictions implied in Tables I and II, one could also look for the effects of thermal diffusivity on high energy sputtering and track registration. For example, in most crystalline dielectric materials, the thermal diffusivity rises very rapidly with decreasing temperature between a few hundred and about ten degrees Kelvin. Thus, a material such as crystalline quartz which registers tracks at room temperature may fail to do so when cooled to a few degrees Kelvin. Some evidence of a dependence of track registration thresholds on thermal conductivity has already been reported.[19,27]

The fact that a fair number of the sputtered particles are charged (probably ~ 10%) and that a condition of LTE appears to prevail inside the target may have important consequences for secondary ion mass spectroscopy (SIMS). For example, Macfarlane et al.[8] have used fission fragments to desorb large quasi-molecular ions from organic compounds which are ordinarily difficult to vaporize without decomposition. With subsequent acceleration and TOF analysis of the ions, they have generated high resolution mass spectra of many non-volatile organic compounds. The line widths of the accelerated ions seem to correspond to a thermal distribution at approximately 60,000 ^{o}K (Reference 28).

6. CONCLUSIONS

We have presented a model for high energy sputtering of dielectric materials which includes a plausable mechanism for rapid heat transfer to the lattice. Despite its simplicity, this "thermalized ion-explosion" model describes the sputtering behavior of UF_4 remarkably well. We feel it is likely that the model can also be used to describe the high energy sputtering of other dielectric materials (such as ice), as well as the phenomenon of track registration.

ACKNOWLEDGMENTS

The authors wish to thank W. L. Brown for suggesting that we look for molecular clusters being sputtered from UF_4.

REFERENCES

1. J. E. Griffith, R. A. Weller, L. E. Seiberling and T. A. Tombrello, Rad. Eff., in press (1980).
2. P. K. Haff, Appl. Phys. Lett. 29, 473 (1976).
3. P. Sigmund, Phys. Rev. 184, 383 (1969).
4. J. P. Biersack and E. Santner, Nucl. Instr. Meth. 132, 229 (1976).
5. W. L. Brown, L. J. Lanzerotti, J. M. Poate and W. M. Augustyniak, Phys. Rev. Lett. 40, 1027 (1978).
6. W. L. Brown, W. M. Augustyniak, E. Brody, B. Cooper, L. J. Lanzerotti, A. Ramirez, R. Evatt and R. E. Johnson (1980) to be published.
7. R. W. Ollerhead, J. Bottiger, J. A. Davies, J. L'Ecuyer, H. K. Haugen and N. Matsunami (1980) to be published.
8. R. D. Macfarlane and D. F. Torgerson, Inst. J. Mass Spectrom. Ion Phys. 21, 81 (1976).
9. P. Dück, W. Treu, W. Galster, H. Fröhlich and H. Volt (1980) to be published.
10. J. E. Griffith, Ph.D. Thesis, California Institute of Technology (1979).
11. J. E. Robinson and D. A. Thompson, Phys. Rev. Lett. 33, 1569 (1974).
12. L. T. Chadderton, D. V. Morgan, I. McC. Torrens and D. Van Vliet, Phil. Mag. 13, 185 (1966).
13. R. L. Fleischer, P. B. Price and R. M. Walker, J. Appl. Phys. 36, 3645 (1965).
14. M. W. Thompson, Phil. Mag. 18, 377 (1968).
15. R. A. Weller and T. A. Tombrello, Rad. Eff. 37, 83 (1978).
16. R. Gregg and T. A. Tombrello, Rad. Eff. 35, 243 (1978).
17. R. Reif, Fundamentals of Statistical and Thermal Physics (McGraw-Hill Book Co., 1965).

18. G. H. Vineyard, Rad. Eff. 29, 245 (1976).

19. A. Sigrist and R. Balzer, Rad. Eff. 34, 75 (1977).

20. R. L. Fleischer, P. B. Price and R. M. Walker, Nuclear Tracks in Solids (University of California Press, Berkeley, 1975).

21. R. L. Fleischer, P. B. Price and R. M. Walker, Phys. Rev. 156, 353 (1967).

22. H. Bethe, Ann. Physik 4, 443 (1930).

23. H. H. Heckman, E. L. Hubbard and W. G. Simon, Phys. Rev. 129, 1240 (1963).

24. B. L. Schram, F. J. De Heer, M. J. Van der Weil and J. Kistemaker, Physica 31, 94 (1965).

25. F. J. De Heer, J. Schutten and H. Moustafa, Physica 32, 1766 (1966).

26. N. H. Fletcher, The Chemical Physics of Ice (Cambridge University Press, 1970).

27. A. Sigrist and R. Balzer, Helv. Phys. Acta 50, 49 (1977).

28. R. D. Macfarlane and D. F. Torgerson, Phys. Rev. Lett. 36, 486 (1976).

TABLE I

Uranium sputtering yield predictions for ten different beams incident at $\frac{1}{4}$ MeV/amu on UF_4. The conditions implied by Case I and Case II are described in section 4. Measured uranium sputtering yields from UF_4 that are taken from References 1 and 10 are given in the last column.

		S(U atoms/ion)			
			Case II		
Beam	Z_e	Case I	E_b = 0.5 eV	E_b = 0.7 eV	measured
H	0.91	1.5×10^{-5}			
$^4He^+$	1.62	1.5×10^{-3}			$\sim 2 \times 10^{-4}$
Li	2.21	1.7×10^{-2}	1.2×10^{-15}	1.2×10^{-21}	
C	3.59	0.83	0.13	3.4×10^{-2}	
$^{16}O^{+2}$	4.32	3.7	3.0	2.3	3.9 ± 1
$^{19}F^{+2}$	4.66	6.7	6.7	6.7	5.6 ± 1
$^{20}Ne^{+2}$	4.97	11.3	11.6	13.7	11.7 ± 2
S	6.59	108	54	93.5	
Cl	6.83	143	61	110	
Ar	7.06	187	69	125	

TABLE II

Measured H_2O sputtering yields taken from Reference 5, shown with the electronic stopping power of each beam used. In the last column are yields predicted by our model (case I) normalized to best fit the data.

Beam	dE/dx (10^{-15} eV cm^2 per molecule)	S (molecules per ion)	$(4 \times 10^{-4}) \times (dE/dx)^{\frac{1}{4}}$
^{1}H	6.8	0.2 ± 0.04	8.6×10^{-4}
^{1}H	17.1	0.4 ± 0.08	0.034
^{4}He	71	10 ± 2	10.2
^{12}C	189	520 ± 100	510
^{16}O	201	640 ± 130	653

FIGURE CAPTIONS

FIGURE 1. Schematic drawing of the experimental apparatus used to determine the TOF spectrum.

FIGURE 2. TOF spectrum of particles sputtered from a UF_4 target with 4.74 MeV $^{19}F^{+2}$. The sputtered ions were accelerated through +100 volts and lie in the region $TOF/28 \times 10^{-6}$ sec < 16. The sharp peaks at low TOF are displayed in expanded form in the inset, and the expected positions of various singly charged molecular ions are shown. The uncertainty in position of the molecular ions shown is approximately ± 20 amu. The dashed line under the first peak indicates the limiting resolution of the spectrometer, and the dashed line below the TOF spectrum represents the slow neutral particles which wrap around the wheel a second time.

FIGURE 3. Velocity spectrum of neutral uranium sputtered from a UF_4 target with 4.74 MeV $^{19}F^{+2}$. The errors are statistical. The solid curve is Equation (5) with M = 235 amu and T = 3500 ^{o}K, with the normalization chosen to best fit the data. The dashed curve is a superposition of two curves, each having the form of Equation (5), assuming 20% of the uranium comes off as U_2 molecules and 80% as U atoms. Both species are assumed to be at T = 4100 ^{o}K.

FIGURE 4. Sputtering yield values as a function of fluorine beam energy. The numbers beside the data points indicate the

incident fluorine charge state and the error bars correspond to the standard deviations of the measured yields in those cases for which more than one run was performed. The dash-dot curve is dE/dx with the maximum corresponding to $\sim$ 300 eV/Å. The solid and dashed curves are Equations (12a) and (12b), respectively, and are normalized to best fit the data.

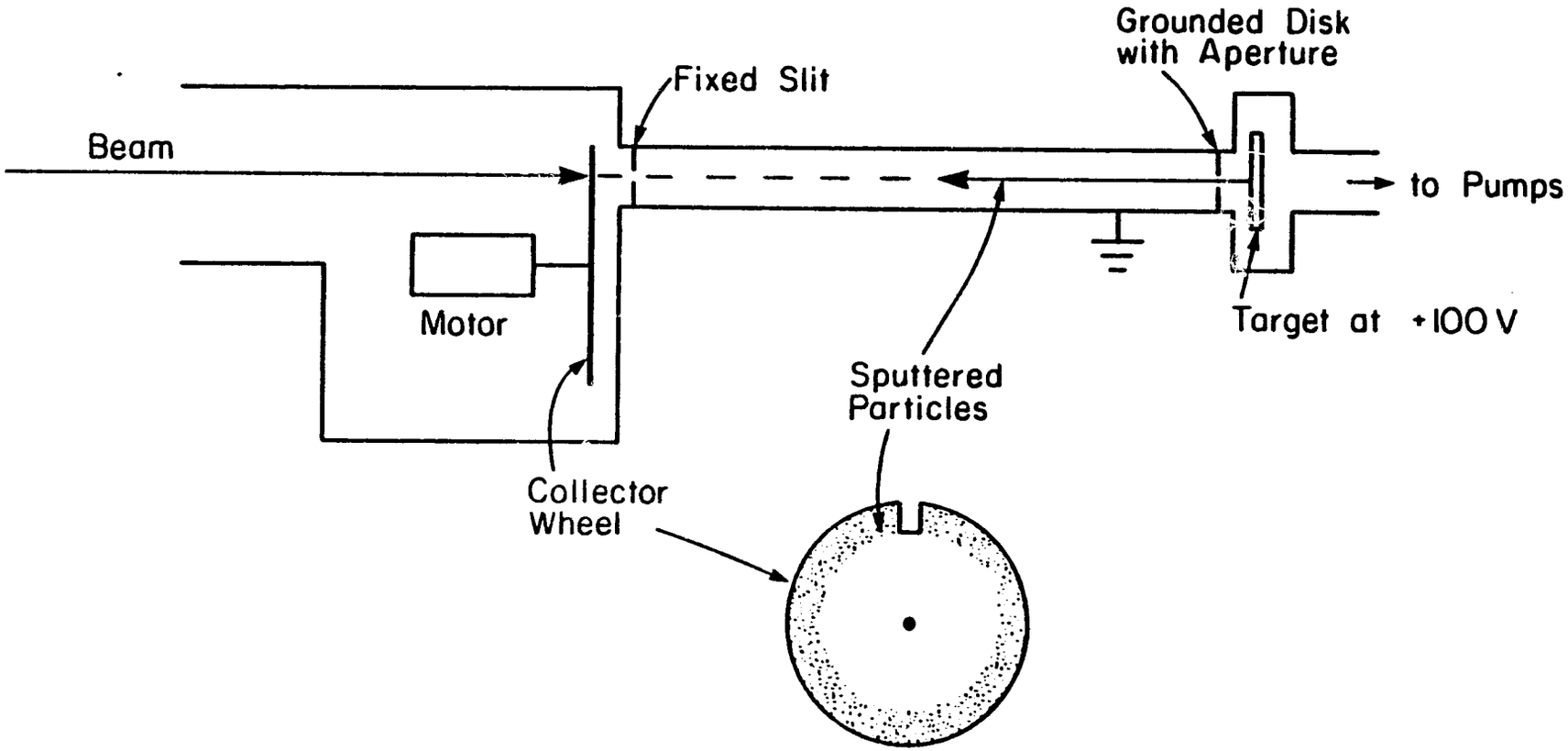
Grounded Disk
with Aperture
Fixed Slit
Beam
to Pumps
Motor
Target at +100 V
Sputtered
Particles
Collector
Wheel

Fig. 1

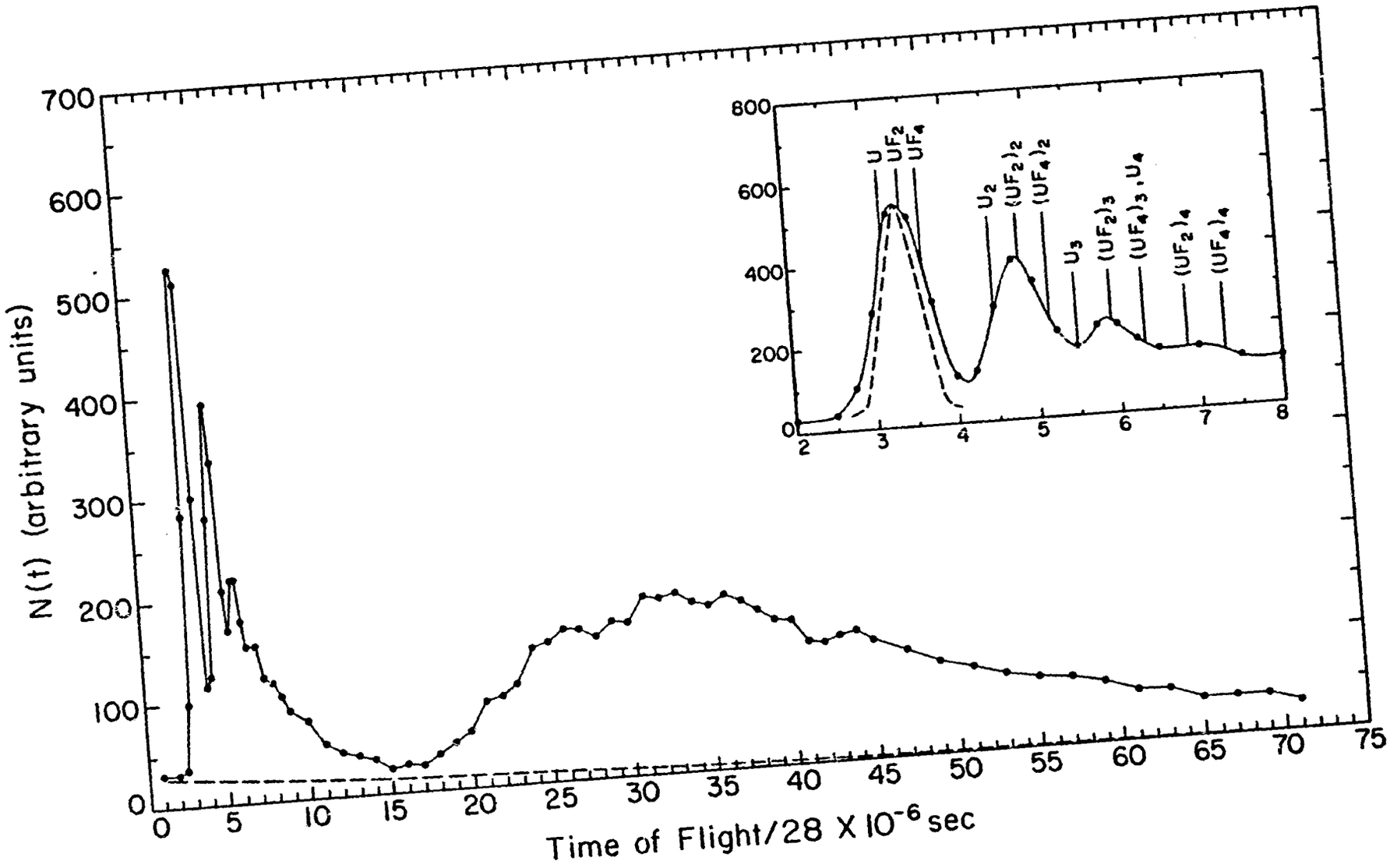
N(t) (arbitrary units)
Time of Flight/28 X 10⁻⁶ sec
U
UF2
UF4
U2
(UF2)2
(UF4)2
U3
(UF2)3
(UF4)3, U4
(UF2)4
(UF4)4

Fig. 2

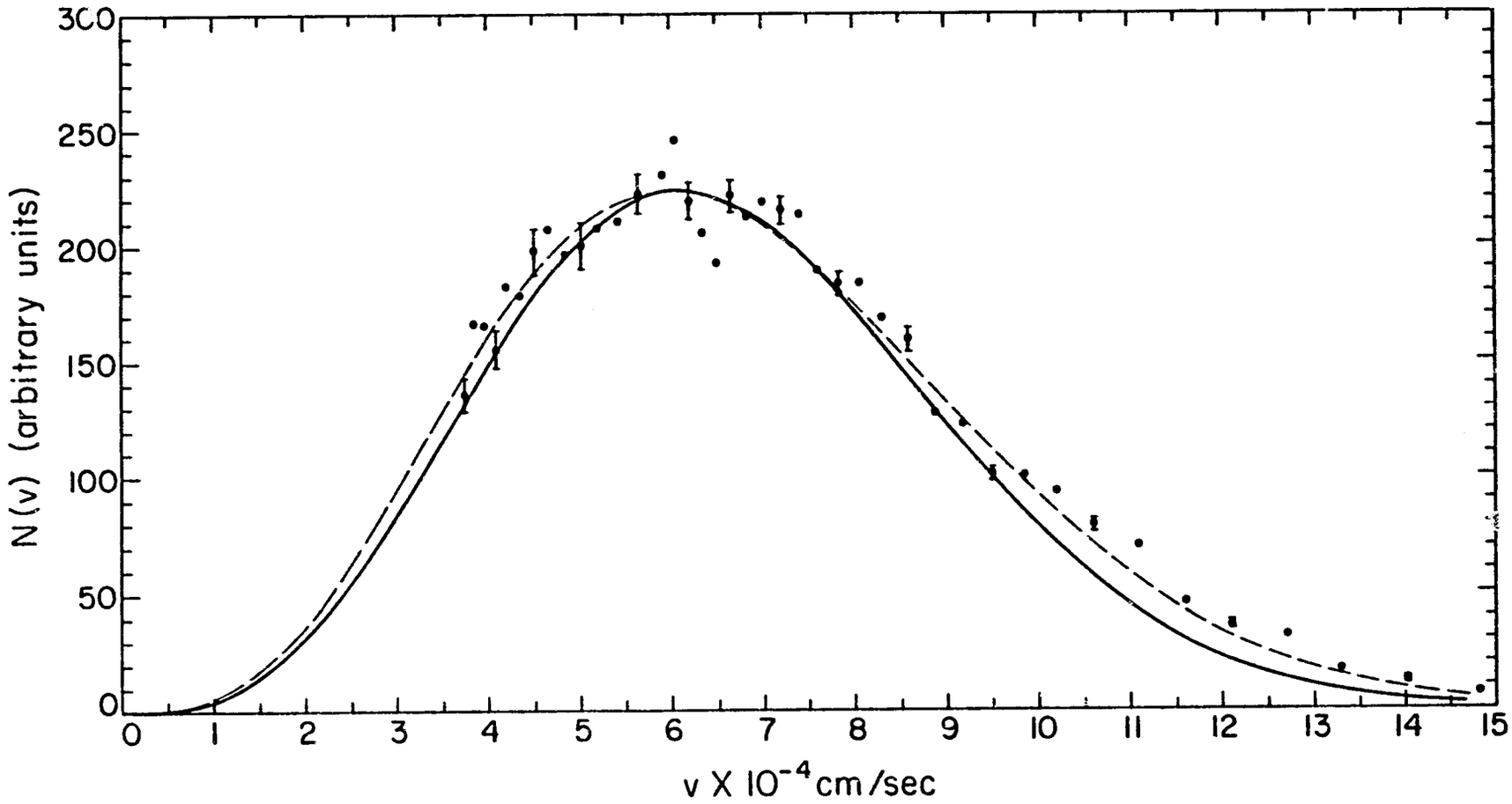
300
250
200
150
100
50
0
N(v) (arbitrary units)
0
1
2
3
4
5
6
7
8
9
10
11
12
13
14
15
v X 10⁻⁴ cm/sec

Fig. 3

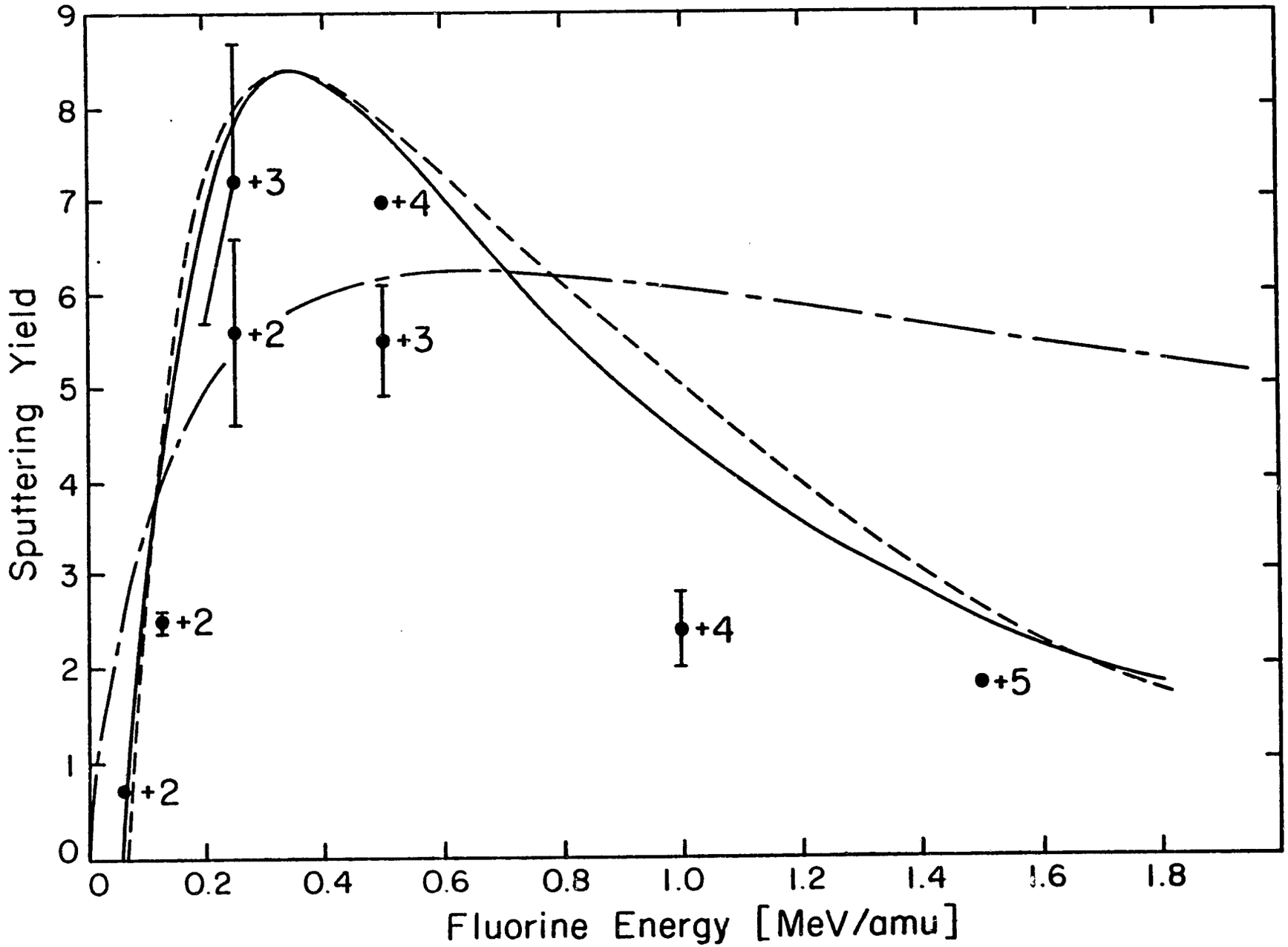
Sputtering Yield
Fluorine Energy [MeV/amu]
0
1
2
3
4
5
6
7
8
9
0
0.2
0.4
0.6
0.8
1.0
1.2
1.4
1.6
1.8
+2
+2
+3
+2
+4
+3
+4
+5

Fig. 4